

Optimization study on the azeotropic distillation process for isopropyl alcohol dehydration

Jungho Cho and Jong-Ki Jeon*[†]

Department of Chemical Engineering, Dong Yang University,
1, Kyochon-dong, Poongki-eup, Youngju, Gyeongbuk 750-711, Korea

*Department of Chemical Engineering, Kongju National University,
182, Shinkwan-dong, Gongju, Chungnam 314-701, Korea
(Received 9 August 2005 • accepted 26 November 2005)

Abstract—Modeling and optimization work was performed using benzene as an entrainer to obtain a nearly pure anhydrous isopropyl alcohol product from dilute aqueous IPA mixture through an azeotropic distillation process. NRTL liquid activity coefficient model and PRO/II with PROVISION 6.01, a commercial process simulator, were used to simulate the overall azeotropic distillation process. We determined the total reboiler heat duties as an objective function and the concentration of IPA at concentrator top as a manipulated variable. As a result, 38.7 mole percent of IPA at concentrator top gave the optimum value that minimized the total reboiler heat duties of the three distillation columns.

Key words: Azeotropic Distillation, Entrainer, NRTL Liquid Activity Coefficient Model, Simulation, Optimization

INTRODUCTION

An anhydrous isopropyl alcohol (IPA) product with purity over 99.9% by weight has been widely used as a raw material of paint or ink products and as a solvent in electronic and medicine industries [Song et al., 2000]. Fundamental physical properties of IPA are listed in Table 1. IPA forms an azeotrope with water at 87.8 wt% and 80.4 °C under normal pressure [Robert et al., 1986]. Therefore, a high-purity IPA product over its azeotropic composition cannot be obtained through conventional distillation because an infinite number of trays are required to reach to the azeotropic point [Holland, 1981]. Many distillation processes have been proposed to separate a pure substance from a mixture [Pradhan and Kannan, 2005; Sahapatsombud et al., 2005]. Among the separation methods to obtain a pure IPA, we focused our attention on the azeotropic distillation process.

There are two kinds of approaches to obtain a nearly pure IPA

using special distillation. One is to utilize an azeotropic distillation process using benzene or cyclohexane as an entrainer [Font et al., 2003; Tao et al., 2003; Al-Amer, 2000; Fele et al., 2000] and the other is an extractive distillation process using ethylene glycol as a solvent [Ligero and Ravagnani, 2003; Pinto et al., 2000]. Fig. 2(a) and (b) show schematic diagrams for an azeotropic distillation column and an extractive distillation column. In azeotropic distillation, by forming a ternary heterogeneous azeotrope lower than any other binary azeotropic temperatures, a nearly pure IPA can be obtained as a bottom product of the azeotropic distillation column. In extractive distillation, by adding a solvent exclusively familiar with water like ethylene glycol, IPA can be obtained as a top product of the extractive distillation column.

Table 1. Fundamental physical properties of IPA

Properties	Value
Chemical formula	C ₃ H ₈ O
Molecular weight (Kg/K-mole)	60.097
Normal boiling point (K)	355.480
Standard liquid density (m ³ /K-mole)	790.22
Critical temperature (K)	508.310
Critical pressure (kPa)	4,734.300
Critical volume (m ³ /K-mole)	0.1670
Critical compressibility factor	0.22000
Acentric factor	0.66615
Heat of formation (kJ/K-mole)	-260,820.00
Free energy of formation (kJ/K-mole)	-168,120.00

[†]To whom correspondence should be addressed.
E-mail: jkjeon@kongju.ac.kr

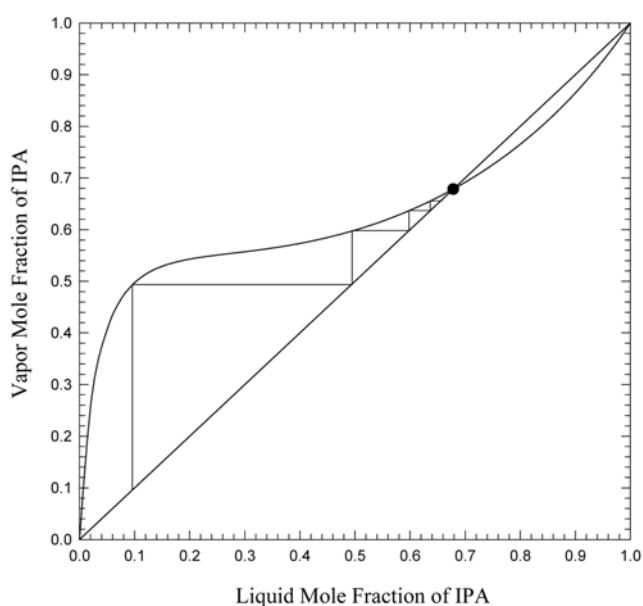


Fig. 1. McCabe-Thiele diagram for the separation of IPA-water binary mixture.

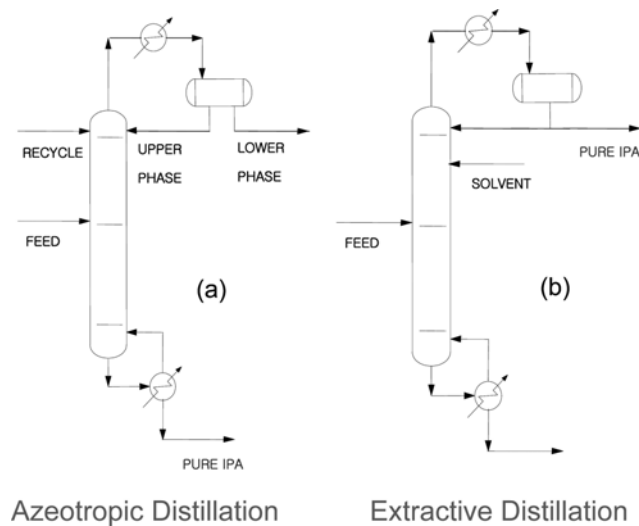


Fig. 2. Two kinds of approaches to obtain a nearly pure IPA product using special distillation, (a) azeotropic distillation column, (b) extractive distillation column.

In this research, modeling and optimization were performed for an IPA azeotropic distillation process using benzene as an entrainer. Fig. 3 shows a schematic diagram for a typical azeotropic distillation process consisting of three distillation columns. The use of the first distillation column is to produce concentrated IPA mixture from a dilute IPA aqueous stream. The second distillation column, which is for azeotropic distillation, can produce a desired IPA product at the bottom of the column when the overhead vapor stream is condensed to cause liquid phase splitting by adding the entrainer. In the third distillation column, a stripper or a dryer, benzene and IPA are stripped to be recycled to the top section of the azeotropic distillation column.

Reasons for selecting benzene as an azeotrope breaking agent are as follows. First, it is to obtain a pure IPA product at the bottom of the azeotropic column by condensing the overhead vapor stream close to the ternary heterogeneous azeotropic point below the other three binary azeotropic temperatures [Perry and Chilton, 1983]. Ac-

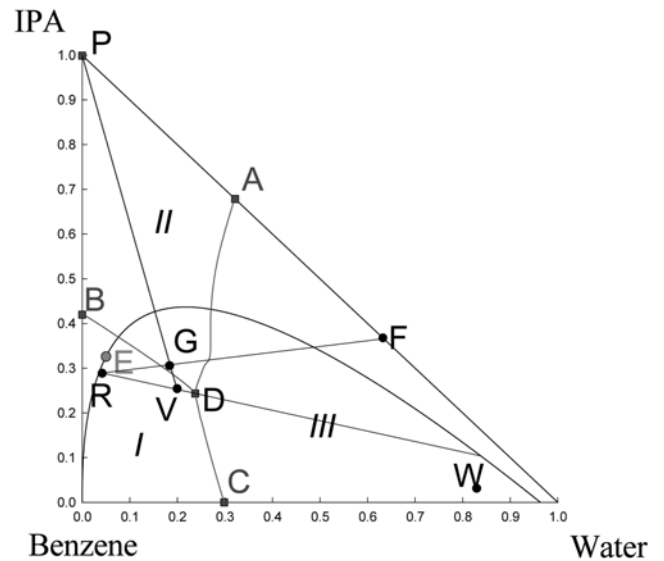


Fig. 4. IPA-water-benzene ternary LLE diagram and distillation curves.

ording to Fig. 4, ternary heterogeneous azeotropic temperature for water-IPA-benzene 65.74°C is lower than the other binary azeotropic temperatures: 78.07°C for ethanol-water azeotrope, 71.53°C for IPA-benzene azeotrope and 69.31°C for water-benzene azeotrope. The second reason for azeotropic distillation is that only mixtures in region II entering to the azeotropic distillation column will produce the desired product of IPA in Fig. 4 [Stanislaw et al., 2000]. A mixture in region III will be separated into pure water instead of pure IPA and the overhead product close to ternary azeotrope. Likewise, any mixture within region I can be separated by simple distillation into pure benzene as a bottom product and a product close to ternary azeotrope at the top of the column.

Even though many other configurations were possible in addition to the process shown in Fig. 3, we focused on modeling based on the scheme above in Fig. 3 and found the optimum solution that minimized the total reboiler heat duties by varying the feed stream concentration to the azeotropic distillation column. We selected IPA

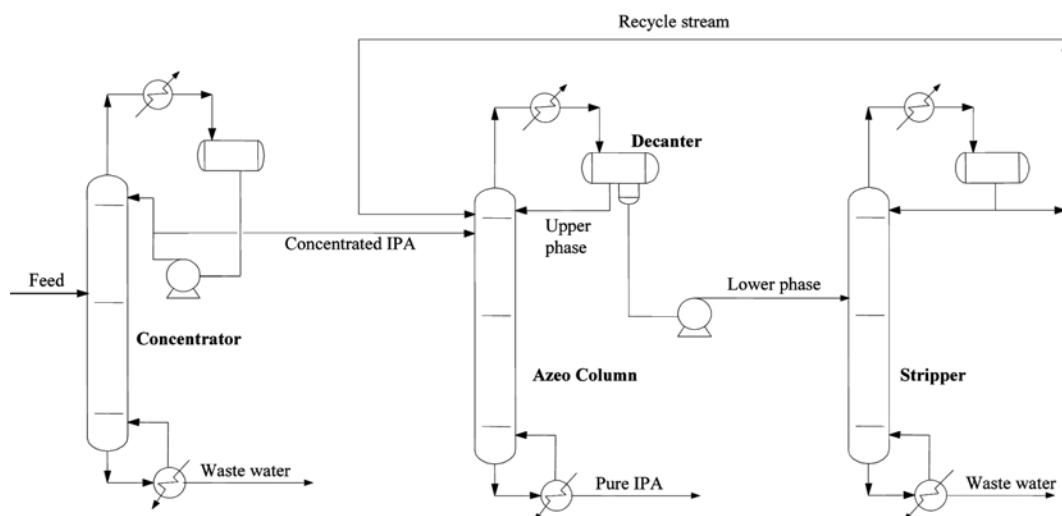


Fig. 3. A schematic diagram for IPA azeotropic distillation process using benzene as an entrainer.

concentration at concentrator top product as a control variable since the concentrator reboiler heat duty increased again very sharply near IPA azeotropic composition with water, whereas reboiler heat duties of the azeotropic distillation column and stripper column decreased slowly.

THEORY

NRTL liquid activity coefficient model [Renon and Prausnitz, 1968] was used to estimate vapor-liquid and liquid-liquid equilibria for azeotropic distillation unit modeling. Liquid activity coefficient for component 'i' in mixture is expressed as:

$$\ln \gamma_i = \frac{\sum_j \tau_{ij} G_{ij} X_j}{\sum_k G_{ki} X_k} + \frac{\sum_j X_j G_{ij}}{\sum_k G_{kj} X_k} \left[\tau_{ij} - \frac{\sum_k X_k \tau_{kj} G_{kj}}{\sum_k G_{kj} X_k} \right] \quad (1)$$

where, τ_{ij} and G_{ij} in Eq. (1) are the optimum binary interaction parameters that minimize deviations from experimental data. τ_{ij} and G_{ij} can be expressed as Eq. (2) and (3).

$$\tau_{ij} = a_{ij} + \frac{b_{ij}}{T} \quad (2)$$

$$G_{ij} = \exp(-\alpha_{ij} \tau_{ij}) \quad (3)$$

In Eq. (2) T refers to absolute temperature, and the NRTL liquid activity coefficient model in Eq. (1) has five regression parameters including a temperature-dependent term for each binary set. Table 2 shows binary adjustable parameters of NRTL model for each binary vapor-liquid and liquid-liquid systems. Table 3 shows the results of a comparison between calculated azeotropic points and temperatures and those obtained through experiment. Binary interaction parameters for binary vapor-liquid equilibria for IPA-water and IPA-benzene systems were optimized with bubble point temperature and vapor composition at given constant pressure (see Eq. (4)) [Gmehling and Onken, 1977]. Binary interaction parameters for binary liquid-liquid equilibria for water-benzene system were regressed with experimental composition both for upper and lower liquid phases (see Eq. (5)) [Macedo and Rasmussen, 1977]. A pattern search optimization algorithm suggested by Nelder and Mead [Nelder and Mead, 1965] was used in regression.

Table 2. NRTL binary interaction parameters for each binary set

Component I	Component J	a_{ij} a_{ji}	b_{ij} b_{ji}	α_{ij}	Units
IPA	Water	0.0000	-267.1320	0.3111	K
		0.0000	461.719		
IPA	Benzene	0.0000	184.511	0.2910	K
		0.0000	366.662		
Water	Benzene	0.0000	665.600	0.2000	K
		0.0000	2,938.000		

$$\text{Obj. (1)} = \left[\sum_{j=1}^N \left(\frac{T_j^{\text{exp}} - T_j^{\text{cal}}}{T_j^{\text{cal}}} \right)^2 + \sum_{j=1}^N \left(\frac{y_j^{\text{exp}} - y_j^{\text{cal}}}{y_j^{\text{cal}}} \right)^2 \right] / N \quad (4)$$

$$\text{Obj. (2)} = \left[\sum_{j=1}^N \left(\frac{X_j^{\text{I,exp}} - X_j^{\text{I,cal}}}{X_j^{\text{I,cal}}} \right)^2 + \sum_{j=1}^N \left(\frac{X_j^{\text{II,exp}} - X_j^{\text{II,cal}}}{X_j^{\text{II,cal}}} \right)^2 \right] / N \quad (5)$$

MODELING OF IPA DEHYDRATION PROCESS USING AZEOTROPIC DISTILLATION

PRO/II with PROVISION release 6.01, a general-purpose chemical process simulator, was used for the simulation of IPA dehydration process using azeotropic distillation. Chemdist algorithm in PRO/II, a Newton-based method suitable for solving non-ideal distillation problems was used to solve azeotropic distillation columns. Fig. 5 is a schematic diagram of an equilibrium stage for the case of two-phase distillation with no chemical reaction. The equations that describe the interior column of the trays are as follows:

$$M_{i,j} = \exp(X_{i,j})L_i + \exp(Y_{i,j})V_i - \exp(X_{i-1,j})(L_{i-1} - L_{i-1}^D) - \exp(Y_{i-1,j})(V_{i-1} - V_{i-1}^D) - f_{i,j}^L - f_{i-1,j}^V \quad (6)$$

$i=1, \text{NT}, j=1, \text{NC}$

$$E_i = L_i \hat{H}_i^L + V_i \hat{H}_i^V - (L_{i-1} - L_{i-1}^D) \hat{H}_i^L - (V_{i-1} - V_{i-1}^D) \hat{H}_i^V - Q_i - F_i^L \hat{H}_i^{FL} - F_{i-1}^V \hat{H}_{i-1}^{FV} \quad (7)$$

$i=1, \text{NT}$

$$Q_{i,j} = Y_{i,j} - X_{i,j} - \ln(K_{i,j}) \quad (8)$$

$i=1, \text{NT}, j=1, \text{NC}$

$$S_i = 1 - \sum_{j=1}^{\text{NC}} \exp(X_{i,j}) \quad (9)$$

$i=1, \text{NT}$

Table 3. Azeotropic compositions and temperatures of binary and ternary systems

Compounds	BP (°C)	Azeotropic temperature (°C)		Weight percent composition					
		exp	cal	In azeotrope		Upper layer		Lower layer	
				exp	cal	exp	cal	exp	cal
a. IPA	82.3	80.4	80.2	87.8	87.6	-	-	-	-
b. Water	100.0			12.2	12.4				
a. Benzene	80.1	71.5	70.6	66.7	64.2	-	-	-	-
b. IPA	82.3			33.3	35.8				
a. Benzene	80.1	69.4	69.3	91.1	91.1	99.94		0.07	
b. Water	100.0			8.9	8.9	0.06		99.93	
a. Benzene	80.1	-		-		-		-	
b. IPA	78.5								
c. Water	100.0								

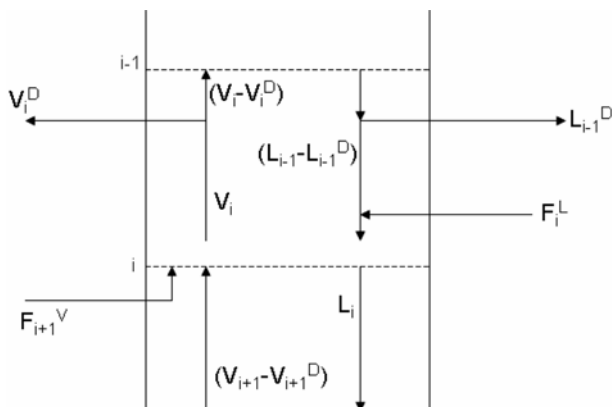


Fig. 5. Schematic of a simple stage for Chemdist algorithm.

Table 4. Feed stream information

Component	Mole%
IPA	10.00
Water	90.00
Temperature (K)	298.15
Pressure (kPa)	300.00
Flow rate (Kmole/hr)	100.00

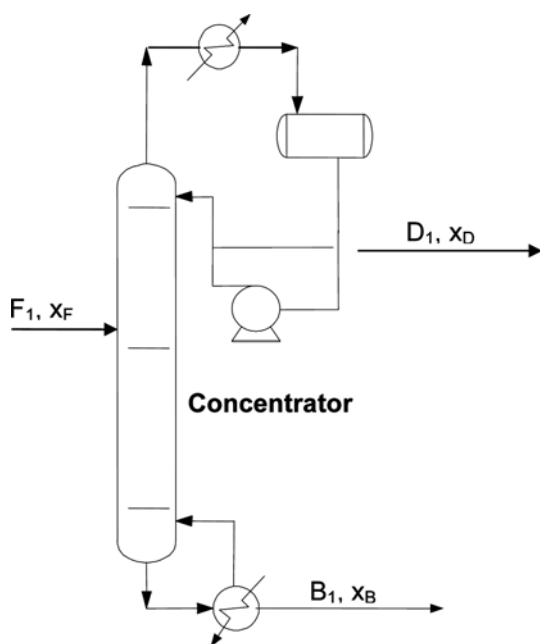


Fig. 6. A schematic diagram of a concentrator.

$$S_i' = 1 - \sum_{j=1}^{NC} \exp(Y_{ij}) \quad (10)$$

$i=1, NT$

Feedstock conditions including composition, temperature, pressure and flow rate are presented in Table 4. Ten mole% of dilute IPA aqueous mixture was fed to the concentrator to obtain pure IPA through a three-column configuration.

1. Concentrator Simulation

Concentrator simulation is basically binary distillation of water

and IPA. However, it is very difficult to get a converged solution since concentrator simulation is highly sensitive to initially guessed values. Fig. 6 shows a schematic diagram of a concentrator. Here, F_1 refers to the molar flow rate of the diluted IPA aqueous solution and x_F refers to the mole fraction of IPA contained in the feed. D_1 , x_D and B_1 , x_B refer to the molar flow rate and the IPA mole fraction at the top and the bottom of the column, respectively. The overall material balance and component material balance for IPA around the concentrator are expressed as Eqs. (11) and (12) below.

$$F_1 = D_1 + B_1 \quad (11)$$

$$F_1 x_F = D_1 x_D + B_1 x_B \quad (12)$$

Since the purpose of the concentrator is to obtain an IPA aqueous stream close to the azeotropic composition as the top product and to produce nearly pure water at the bottom of the column, we can assume that x_B is almost equal to zero and x_D is around an azeotropic composition of 0.68. Thus, Eq. (12) above can be rewritten as Eq. (13).

$$D_1 = F_1 \times \frac{x_F}{x_D} \cong F_1 \times \frac{x_F}{x_{azeo}} = 100 \times \frac{0.10}{0.68} \cong 14.71 \quad (13)$$

The theoretical number of trays for the concentrator was fixed at 30.

2. Decanter Simulation

Decanter simulation, which is fundamentally for calculating liquid-liquid equilibrium, is very important because it gives proper initially guessed values in order to obtain a converged solution of azeotropic distillation column. Fig. 7 shows a schematic diagram of a decanter. V , R and W in Fig. 7 are the same as those in Fig. 2. V , R and W refer to the azeotropic column overhead vapor composition and the

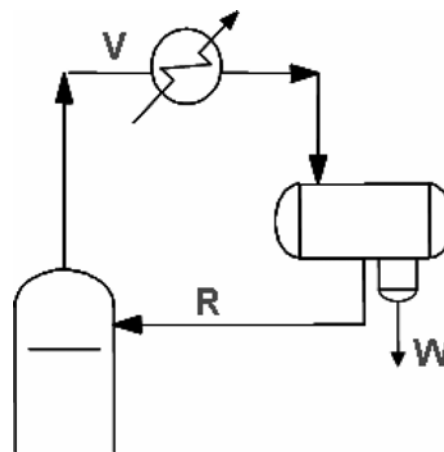


Fig. 7. A schematic diagram around a decanter.

Table 5. Material balance around decanter

	V (mole fraction)	R (mole fraction)	W (mole fraction)
Benzene	0.2000	0.0048678	0.4586
IPA	0.2500	0.1614	0.3674
Water	0.5500	0.8337	0.1740
Molar fraction	1.0000	0.5700	0.4300

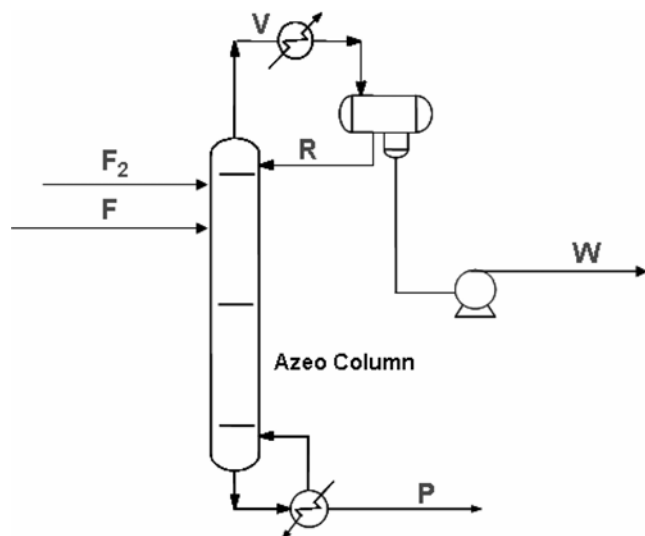


Fig. 8. A schematic diagram of an azeotropic distillation column.

upper and lower liquid phase stream compositions in decanter, respectively. Table 5 shows material balances around the decanter.

3. Simulation of Azeotropic Distillation Column

Fig. 8 shows a schematic diagram for an azeotropic distillation column. Here, D_1 refers to the concentration of a concentrated IPA stream fed to the azeotropic distillation column, and F_2 refers to the concentration of IPA stream recycled to the azeotropic distillation column. The total molar flow rate of water entering to the azeotropic distillation column can be written as Eq. (14).

$$\begin{aligned} \text{Total water feed rate to azeo column} &= 14.17 \times (1 - 0.68) + N_{\text{Recycle}} \times (1 - 0.68) \\ &= 4.5344 + 0.32N_{\text{Recycle}} \end{aligned} \quad (14)$$

In Eq. (14) above, the total molar flow rate of water fed to the azeotropic distillation column is equal to the total water flow rate at the aqueous phase stream of the decanter because a nearly pure IPA should be obtained as the product at the bottom of the azeotropic column. Therefore, we can rewrite the total water molar flow rate coming out from the decanter as Eq. (15) below.

$$N_w = N_f \times 0.4586 \times 0.4300 = 0.1972N_f \quad (15)$$

Combining Eq. (14) and (15), a material balance for water around the azeotropic distillation column can be obtained by Eq. (16) below.

$$0.1972N_f = 4.5344 + 0.32N_{\text{Recycle}} \quad (16)$$

In a similar way, the material balance for IPA around the azeotropic distillation column is expressed as Eq. (17).

$$N_{\text{Recycle}} = (0.3764)(0.43)N_f = 0.1580N_f \quad (17)$$

Combining Eqs. (16) and (17), we can get solutions 30.92 for N_f and 4.8848 for N_{Recycle} . Initially guessed values obtained from a series of equations from Eqs. (11) to (17) above can be helpful to get a converged solution easily. We set the number of theoretical trays for the azeotropic distillation column at 30.

4. Stripper Simulation

Modeling the simulation of a stripper is relatively simple. For the first specification the reflux ratio was fixed at 1.5, and for the second specification the IPA content at the bottom of the stripper

column was set at 1.0 mole%. We also varied the heat duties of the condenser and the reboiler to meet the two product specifications above.

RESULTS AND DISCUSSION

Modeling and optimization processes for an overall azeotropic distillation unit can be understood best by the IPA-water-benzene ternary LLE diagram and distillation curves illustrated in Fig. 4. Fig. 4 shows an IPA-water-benzene ternary LLE phase diagram at decanter operating temperature of 45 °C. Here, points A, B, C and D refer to IPA-water, IPA-benzene, water-benzene binary azeotropes and IPA-water-benzene ternary azeotrope, respectively. Point D refers

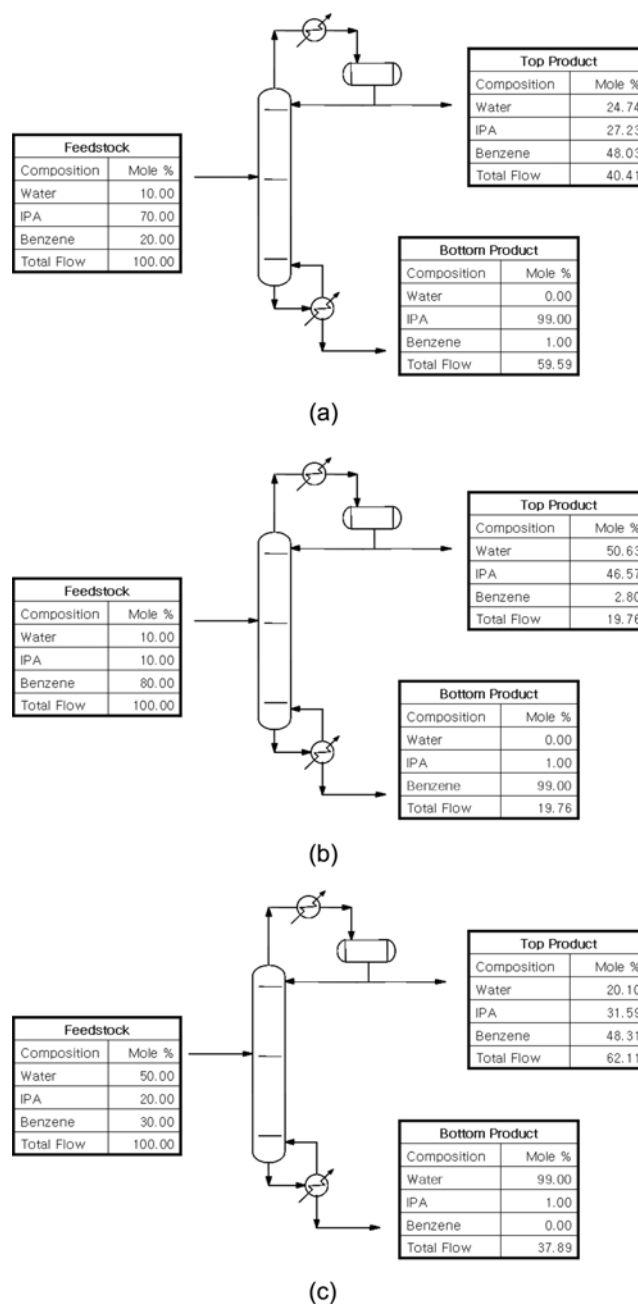


Fig. 9. Bottom products for three feedstock compositions.

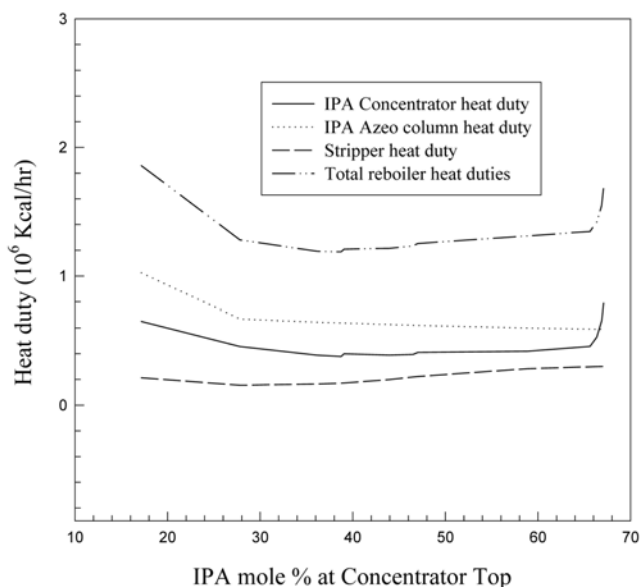


Fig. 10. Heat duties versus IPA mole percent at concentrator top.

to the plait point where liquid-liquid two phases are merged into a single liquid phase. Point F is the overall composition fed to the azeotropic column. Curves AD, BD and CD divide the ternary LLE diagram into three parts, region I, II and III. According to Fig. 9(a), only mixtures in region II can produce desired product composition, namely, nearly pure IPA at the bottom of the azeotropic column. If the overall composition is within region I in Fig. 9(b), pure benzene will be obtained instead of pure IPA. Similarly, mixtures in region III in Fig. 9(c) will produce pure water at the bottom of the column. In Fig. 4, line RF refers to the sum of compositions fed to the azeotropic column and line VP refers to the sum of compositions coming out from the azeotropic column. According to a component mass balance, G the intersection of line RF and VP becomes the overall composition fed to the azeotropic distillation column. Fig. 4 shows that, because overall composition G is within region II, nearly pure IPA can be obtained at the bottom of the azeotropic distillation column as well as overhead vapor composition V close to ternary azeotropic composition as the overhead vapor of the azeotropic column.

Modeling and optimization were performed to produce over 99.9 mole% of IPA stream from a dilute IPA aqueous stream. Fig. 10 shows the heat duty of each reboiler and the total heat duty of the reboilers according to the purity of IPA at the top of the concentrator. In the concentrator, along with the increase of the purity of IPA, the heat duty of a reboiler decreases slowly and again increases and increases rapidly at around 66 mole% of IPA. In the azeotropic distillation column, the heat duty of a reboiler decreases slowly as the concentration of IPA at the top of the concentrator increases. The reason why the heat duty of a stripper reboiler slightly increases with the increase of the concentration of IPA at the top of the concentrator is that the total water flow rate to the stripper increases with the increase of the concentration of IPA at the top of the concentrator. The optimum mole% of IPA at the top of the concentrator that minimizes the objective function is 38.7 and the optimum value of objective function is 1.1876×10^6 Kcal/hr.

CONCLUSION

In this study, modeling and optimization were performed separately to obtain over 99.9 mole% of IPA from a dilute IPA aqueous stream using benzene as an entrainer through an azeotropic distillation process. The NRTL liquid activity coefficient model was used to simulate the overall azeotropic distillation unit. This research proved that the optimum concentration of IPA at the top of the concentrator that minimizes the total heat duty of reboilers is 38.7 mole%.

ACKNOWLEDGMENTS

This work was supported by grant number (R01-2002-000-00098-0) from the basic research program of the Korea Science and Engineering Foundation.

NOMENCLATURE

- T : absolute temperature [K]
- F_1 : feed flow rate to concentrator
- D_1 : concentrator top flow rate
- B_1 : concentrator bottom flow rate
- V : azeotropic column overhead vapor composition
- R : decanter upper phase liquid composition
- W : decanter lower phase liquid composition
- $N_{Recycle}$: recycle stream composition to azeotropic column from stripper
- N_W : composition of aqueous stream at decanter bottom
- N_V : composition at azeotropic column overhead vapor stream
- F_i : total feed flow to tray i
- L_i : total liquid flow from tray i
- V_i : total vapor flow from tray i
- Q_i : heat added to tray i
- T_i : temperature of tray i
- $X_{i,j}$: $\ln(x_{i,j})$, natural log of the liquid mole fractions
- $Y_{i,j}$: $\ln(y_{i,j})$, natural log of the vapor mole fractions
- T_j^{exp} : experimental bubble point temperature
- T_j^{cal} : calculated bubble point temperature
- y_j^{exp} : experimental bubble point composition
- y_j^{cal} : calculated bubble point composition
- $x_j^{I,exp}$: experimental liquid phase composition of phase I
- $x_j^{I,cal}$: calculated liquid phase composition of phase I
- $x_j^{II,exp}$: experimental liquid phase composition of phase II
- $x_j^{II,cal}$: calculated liquid phase composition of phase II
- NC : number of components
- NT : number of trays
- N : number of experimental data points
- x_F : dilute IPA mole fraction
- x_D : IPA mole fraction at concentrator top
- x_B : IPA mole fraction at concentrator bottom
- x_{azeo} : mole fraction of IPA at azeotrope
- Obj.(1) : objective function 1
- Obj.(2) : objective function 2
- γ_i : activity coefficient of component i
- x_j, x_k : liquid mole fraction of component j and k
- $a_{ij}, a_{ji}, b_{ij}, b_{ji}, \alpha_{ij}$: binary interaction parameter in van der Waals mixing rule

REFERENCES

- Al-Amer, A. M., "Investigating polymeric entrainers for azeotropic distillation of the ethanol/water and MTBE/methanol systems;" *Industrial and Engineering Chemistry Research*, **39**, 3901 (2000).
- Fele, L., Stemberger, N. Z. and Grilic, V., "Separation of water+(*o*-, *m*-, *p*-) xylene systems;" *Journal of Chemical Engineering Data*, **45**, 784 (2000).
- Font, A., Asensi, J. C., Ruiz, R. and Gomiz, V., "Application of isoocane to the dehydration of ethanol. Design of a column sequence to obtain absolute ethanol by heterogeneous azeotropic distillation;" *Industrial and Engineering Chemistry Research*, **42**, 140 (2003).
- Gmehling, J. and Onken, U., *Vapor-liquid equilibrium data collection. aqueous-organic systems, chemistry data series*, Vol. I, Part 1, DECHEMA (1977).
- Holland, C. D., *Fundamentals of multicomponent distillation*, McGraw-Hill (1981).
- Ligero, E. L. and Ravagnani, T. M. K., "Dehydration of ethanol with salt extractive distillation-a comparative analysis between processes with salt recovery;" *Chemical. Engineering and Processing*, **42**, 543 (2003).
- Macedo, E. A. and Rasmussen, P., *Liquid-liquid equilibrium data collection, supplement 1, chemistry data series*, Vol. V, Part 4, DECHEMA (1987).
- Nelder, J. A. and Mead, R. A., "A simplex for function minimization;" *Computer Journal*, **7**, 303 (1965).
- Pradhan, S. and Kannan, A., "Simulation and analysis of extractive distillation process in a valve tray column using the rate based model;" *Korean J. Chem. Eng.*, **22**, 441 (2005).
- Perry, R. H. and Chilton, C. H., *Chemical engineer's handbook 15th edition*, McGraw-Hill (1983).
- Pinto, R. T. P., Wolf-Maciél, M. R. and Lintomen, L., "Saline extractive distillation process for ethanol purification;" *Computers and Chemical Engineering*, **24**, 1689 (2000).
- Renon, H. and Prausnitz, J. M., "Local composition in thermodynamic excess functions for liquid mixtures;" *AIChE J.*, **14**, 135 (1968).
- Robert, C. W., Melvin, J. A. and William, H. B., *CRC handbook of chemistry and physics*, 67th edition, CRC press (1986).
- Sahapatsombud, U., Arpornwichanop, A., Assabumrungrat, S., Praserttham, P. and Goto, S., "Simulation studies on reactive distillation for synthesis of tert-amyl ethyl ether;" *Korean J. Chem. Eng.*, **22**, 387 (2005).
- Song, J. S., Kang, T. I. and Park, S. J., "Phase behavior of IPA-water-entrainer and process design on IPA azeotropic distillation process;" *HWAHAK KONGHAK*, **38**, 633 (2000).
- Stanislaw, K. W., Leo, C. K. and Francisco, J. L. C., "Optimal design of complex azeotropic distillation columns;" *Chemical Engineering Journal*, **79**, 219 (2000).
- Tao, L., Malone, M. F. and Doherty, M. F., "Synthesis of azeotropic distillation with recycles;" *Industrial and Engineering Chemistry Research*, **42**, 1783 (2003).